PAPER L

A STUDY OF ACOUSTIC WAVE EQUATION TOMOGRAPHY APPLIED TO ANELASTIC SYNTHETIC DATA THAT INCLUDES BOREHOLE EFFECTS

Feng Yin and Youli Quan

ABSTRACT

In order to understand the inversion property of wave equation tomography when it is applied to real data, we used a synthetic elastic wave field with attenuation to better simulate the real wave field recorded in real cross well experiments. We used the simulation method described in the paper (Quan, Chen, and Harris, 1995). However, we apply our *acoustical* wave equation tomography method in the frequency domain to this synthetic data set to study the inversion properties, for example, its robustness, the relationship between artifact and noise (e.g., S wave, converted wave, etc.) in the wavefield, borehole effects on the inversion, etc.. This work shows that the resolution of acoustical equation tomography is higher than traveltime tomography as predicated by the theory, and the artifacts in the image can be controlled in an acceptable way if we can accurately extract the scattered field. We believe that the borehole elastic wave modeling method (Quan, et al, 1995) is very useful for testing the inversion property of acoustic wave equation tomography before it is applied to a real dataset.

INTRODUCTION

Acoustical wave equation tomography methods for cross well imaging have been studied for many years. Presently, they are being applied to real data (Harris and Wang, 1993, Song et al., 1995, Zhou, et al, 1995). But the real data usually are recorded in the anelastic media between cased boreholes. When we apply the acoustic wave equation tomography methods to this kind of data, it is hard for us to understand the properties of our simplified model based on our acoustic wave equation when it is applied to real data usually involving S waves, converted waves, casing effects, and radiation patterns, etc. Therefore, we wish to apply acoustical wave equation tomography to the synthetic elastic wave field with attenuation in cased boreholes before we apply them to real data. The literature is limited in this area. The possible reasons are that the methods which are able to simulate the wave field recorded in two dimensional inhomogenous anelastic media between cased boreholes have not been well developed. Fortunately, a method which can simulate the wave field in radially layered media with horizontal structures between cross well with casing has been developed in this year (Quan, Chen and Harris, 1995). Therefore, we can utilize this method to produce the synthetic elastic wave field with attenuation between cased borehole, and apply our acoustic wave equation tomography method to the synthetic dataset to test its inversion properties. Then we can analyze the factors which affect the quality of our imaging method: its robustness, the relationship between inversion artifacts and noise in the wavefield, the error of estimating source function, borehole effects on the inversion, etc.

We first studied the application of acoustic wave equation tomography to the anelastic synthetic data without wavefield separation. We also tested the accuracy and robustness of the codes for elastic forward modeling. We found that it is possible to apply wave equation tomography to the elastic wave field and the inversion artifacts can be controlled to an acceptable level if we can accurately obtain the scattered wave field. The resolution is much higher than travel time tomography. The results show that the method and code for elastic waves modeling in radially layered media with horizontal structure is very useful and helpful for testing the inversion property of the wave equation tomography based on the acoustical equation.

THE TEST OF WAVE EQUATION TOMOGRAPHY APPLIED TO ANELASTIC SYNTHETIC DATA

1. Wave Field Imaging and Travel Time Tomography method

The imaging method we used is based on the acoustical equation in the frequency domain. We have

$$(\nabla^2 + \frac{\omega^2}{c^2(\boldsymbol{r})})U_t(\boldsymbol{r},\omega) = -\delta(\boldsymbol{r} - \boldsymbol{r}_s) \qquad (1)$$

where, $c(\boldsymbol{r})$ is the velocity of the compression wave, $\boldsymbol{r}$ is the position vector, $\boldsymbol{r_s}$ the source position, $U_t(\boldsymbol{r},\omega)$ is the pressure field, and ω is the angle frequency. The scattered wave field is expressed as

$$U(r_s,r_g) = -\omega^2 \iint dx G(\boldsymbol{r},\boldsymbol{r}_g,\omega) O(\boldsymbol{r}) U_t(\boldsymbol{r},\boldsymbol{r}_s,\omega) d\boldsymbol{r} \qquad (2)$$

where $O(\boldsymbol{r}) = \frac{2\delta v(\boldsymbol{r})}{v(\boldsymbol{r})}$, $U(r_s,r_g)$ is the measured scattered field. The goal of the inversion can be reached by minimizing a representative objective function. In this paper an l_2 norm of the data residuals is used as the objective function. Then the gradient direction can be used in iterative optimization methods to minimize the objective function (Harris and Yin, 1994).

The gradient of the objective function $Q(\boldsymbol{m})$ with respect to the model space $\boldsymbol{m}$ can be derived as

$$g = \frac{1}{2}\frac{\partial Q}{\partial m} = -\frac{2\omega 2}{v(r)^3}\sum_{s,g}[G(\boldsymbol{r},\boldsymbol{r}_g,\omega) * U_t(\boldsymbol{r},\boldsymbol{r}_s,\omega)]^* \delta U(\boldsymbol{r}_s,\boldsymbol{r}_g,\omega) \qquad (3)$$

The simplest way for updating the current model can be obtained from

$$v_{i+1} = v_i + \beta * \delta v \qquad (4)$$

where δv = g, and β is a damping factor.

In the travel time tomography, the method we used is the combination algorithm of ART and SIRT.

2. Numerical Experimental setup and results

Figure 1(a) shows the cross-well imaging system, including a cased borehole filled with water. Between the wells, there is a 2-D inhomogeneous body with a fault embedded in a homogeneous background with a P wave velocity of 5000 m/s, S wave velocity of 2900 m/s ,and a Q value of 300. The P wave velocity of the inhomogeneous body is 5800 m/s and the S wave velocity is 3300 m/s, and the Q value is 300. The model used for forward modeling and imaging is shown by Figure 1(b). The cased well contains 51 sources and the other well is the receiver well which contains 51 receivers. The vertical spacing of the source and receiver is 2 meters. The distance between the source and receiver well is 60 meters. We use the method and codes described in another paper (Quan, Chen and Harris, 1995) to produce a synthetic elastic wave field recorded in the horizontal direction, which is the total field. Then we remove the inhomogeneous body and produce a synthetic wave field recorded in the horizontal direction, which is the incident field. We derive the scattered field by subtracting the incident field from the total field.

We transformed the waveforms from the time domain to the frequency domain from the numerical synthetic scattered dataset to obtain the wave field in frequency domain. The figure 1(c) shows the real part of the scattered wave field in the frequency domain with frequency of 300 Hz in which the x direction is receiver line and z direction are source line. Then we picked one source gather from the synthetic seismogram datasets. Figures 2 (a), (b) and (c) are one source gather of the seismograms of the total field, the incident field, and the scattered field, respectively.

Then, we used the imaging methods described in the section (2) to conduct wave field imaging and travel time tomography. The reconstruction of the object in the slowness map are shown in figure 3, in which the figure 3(a) is the reconstructed result using one frequency of 300 Hz; figure 3(b) is the result using 5 frequencies at 233, 266, 299, 332, 365 Hz together; figure 3(c) is the travel time tomogram using the combination algorithm of ART and SIRT. From the imaging result and test, we derived following conclusions.

CONCLUSIONS

We have studied the application of acoustical wave equation tomography to the elastic wave field with attenuation in a simple model including a well with casing. With this simply model, we find that the artifacts due to converted wave and S wave and tube wave can be controlled under an acceptable level if we can derive an accurate scattering wave field. The resolution of wave equation tomography is much higher than travel time tomography as predication by theory analysis. The results show that the method and codes used to simulate the elastic wave with attenuation are helpful to test the property of our wave equation tomography before they are applied to real data. In the future, we will continue to test various factors which will affect the quality of the tomogram. This include the error of extracting the scattered wave field, error of estimating the source function, radiation pattern effect in more complicated models. We will continue to develop more accurate and fast acoustical modeling method, for arbitrary 2 dimensional inhomogeneous media to be used in acoustical wave equation tomography

ACKNOWLEDGMENTS

The work is supported by the Seismic Tomography Project of Stanford University, a research consortium sponsored by companies of the oil and gas industry. We would like to thank Nicholas Smalley for his help in editing this report.

REFERENCES

Harris Jerry M. and Gang Wang, Diffraction tomography for inhomogeneities in a layered background, Expanded Abstract of 63rd Anuual meeting of SEG, 49-52, 1993.

Harris Jerry M. and Feng Yin, Nonlinear multi-frequency wave equation tomography, Expanded Abstract of 64rd Anuual meeting of SEG, 988-991, 1994.

Quan Youli, Xiaofei Chen and Jerry M. Harris, Synthetics of elastic waves in radially layered media with horizontal structures, STP report 95 in this volume.

Song Z.M. and P. R. Williamson, and R.G. Pratt, Frequency-domain acoustical-wave modeling and inversion of crosshole data, Part2 - Inversion method, synthetic experiments, and real data results, Geophysics, 796-809, 1995

Zhou C., W. Cai, Y. Luo, G.T., Schuster, and S. Hassanzadeh, Acoustical wave equation traveltime and waveform inversion of crosshole seismic data, 765-773, Geophysics, Vol. 60, No. 3, 1995

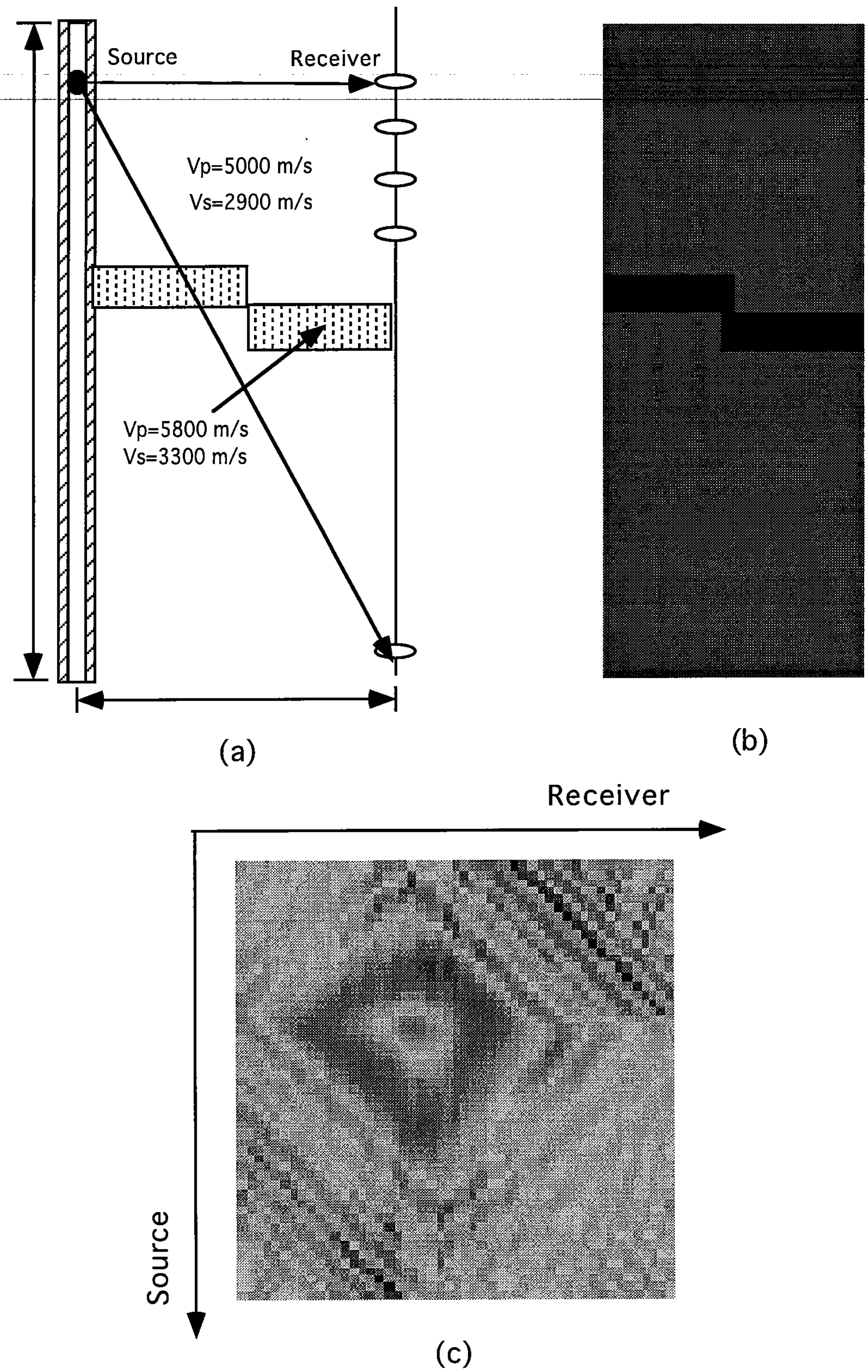

Figure 1 (a) The Cross well numerical experiment Geometry
(b) A fault Model for numerical test
(c) Scattering wave field in frequency domain

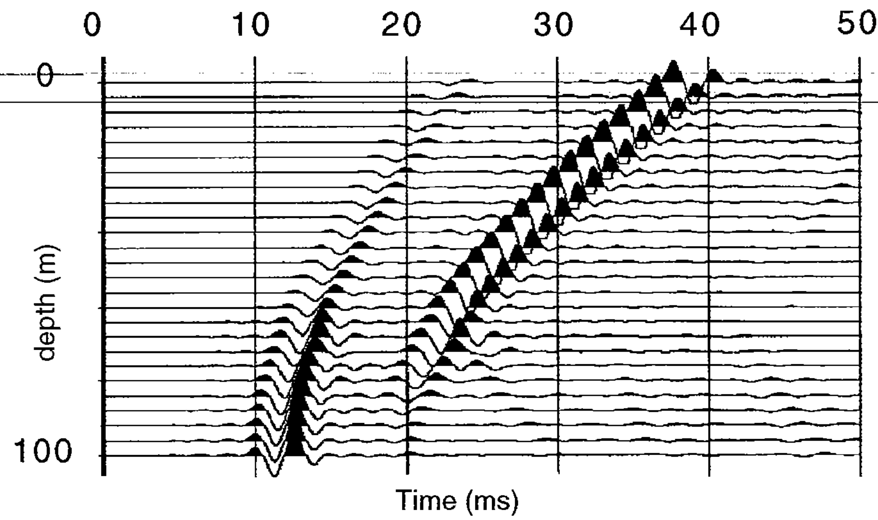

(a)

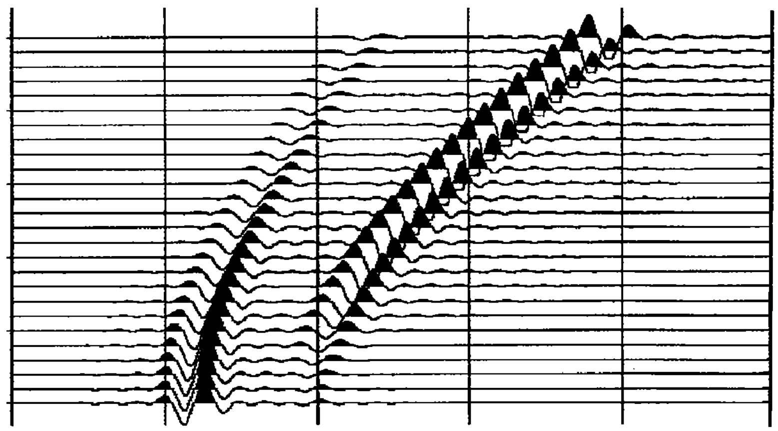

(b)

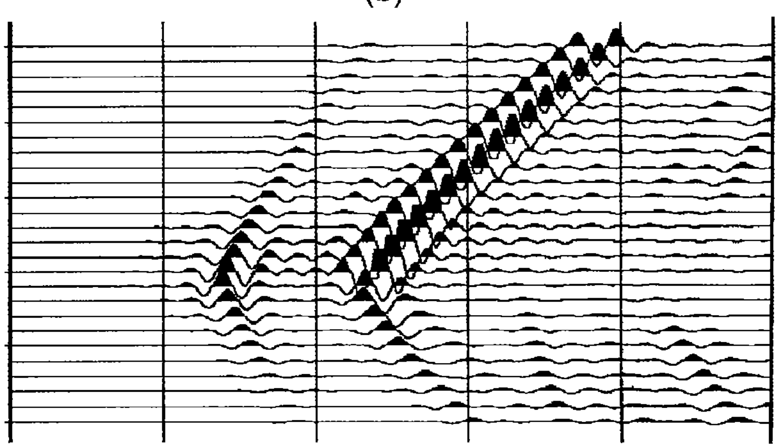

(c)

Figure 2: (a) One source gether of the elastic total wave field in cross well geometry shown by Figure 1
(b) One source gether of the elastic incident wave field
(c) One source gether of the elastic scattering field

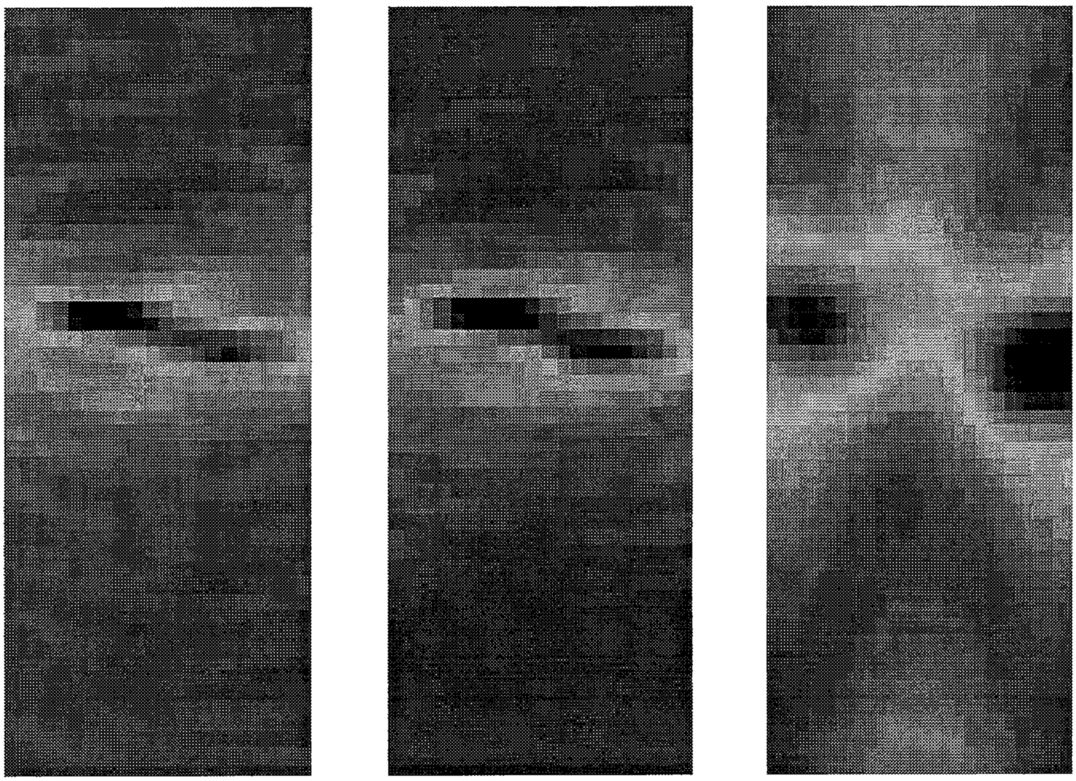

(a) (b) (c)

Figure 3: (a) Wave Field Backpropagation Imaging using scattering sfield shown by Figure 1 (c), the frequency = 300 Hz

(b) Wave field backpropagation imaging using multi-frequencies wave field, the frequency band is 233 - 365 Hz.

(c) Travel Time tomography derived by ART and SIRT together in which the iterations of ART and SIRT are 30, 40, respectively